

RESEARCH

Open Access



Comprehensive sinus contour classification and its characteristics from radiographic examination: a cross-sectional study

Xi Lin¹, Shaobing Li¹, Xianghui Zheng² and Guoying Que^{2*}

Abstract

Objective The aim of this study was to propose a comprehensive maxillary sinus (MS) contour classification system based on the evaluation of anatomical characteristics from cone beam computed tomography (CBCT) examination and investigate the relationship between sinus contours and sinus floor elevation (SFE).

Methods A total of 283 CBCT scans from patients who had single tooth loss in the posterior maxilla and underwent SFE were analyzed. The MS was classified at each tooth position. For buccal-palatal evaluation, the classification from Type A to E was narrow-taper, taper, ovoid, square, and irregular, respectively. For mesial-distal evaluation, the classification from Type 1 to 4 was flat, slope, concave, and septa, respectively. The major anatomical parameters evaluated were (1) residual bone height (RBH), (2) sinus width (SW), (3) maxillary sinus angle (MSA), (4) buccal dip angle (BDA), (5) palatonasal recess (PNR), and (6) sinus depth.

Results Eleven groups of MS contour were classified after detailed calculation. Differences in the RBH, MSA, BDA, and SW among different groups were statistically significant. The narrow-taper and slope MS (A2) group had the highest RBH (8.66 ± 0.77 mm), largest BDA ($79.9^\circ \pm 3.18^\circ$), smallest MSA ($19.8^\circ \pm 2.01^\circ$), and narrowest SW (6.30 ± 1.23 mm). The lowest RBH was in the square and concave sinus (D3) group (5.11 ± 2.70 mm). The ovoid and concave sinus (C3) group had the smallest BDA (50.64 ± 8.73 mm) and largest MSA ($74.11^\circ \pm 11.52^\circ$). The square and flat MS (D1) group had the widest SW (19.13 ± 3.69 mm). A strongly significant positive correlation was observed between the SW and MSA ($r=0.67$) and a strongly negative correlation between the SW and BDA ($r=-0.65$). The prevalence of PNR (mean angle: $104.06^\circ \pm 16.83^\circ$, mean height: 14.72 ± 11.78 mm) was 38% and frequently observed in the ovoid and slope MS (C2) group.

Conclusion Despite certain characteristics at different tooth sites, the same tooth position was categorized differently using different classification systems, indicating large anatomical variations in the MS. The classification system proposed herein allows for classification based on general characteristics at a single tooth site, aiming to help surgeons in improving presurgical evaluation.

Keywords Maxillary sinus, Anatomy, Cone beam computed tomography, Morphology

*Correspondence:
Guoying Que
2917268593@qq.com

¹Affiliated Implantology center, Stomatological Hospital, School of Stomatology, Southern Medical University, Guangzhou, People's Republic of China

²Affiliated Stomatological Hospital, School of Stomatology, Southern Medical University, Guangzhou, People's Republic of China



© The Author(s) 2024. **Open Access** This article is licensed under a Creative Commons Attribution-NonCommercial-NoDerivatives 4.0 International License, which permits any non-commercial use, sharing, distribution and reproduction in any medium or format, as long as you give appropriate credit to the original author(s) and the source, provide a link to the Creative Commons licence, and indicate if you modified the licensed material. You do not have permission under this licence to share adapted material derived from this article or parts of it. The images or other third party material in this article are included in the article's Creative Commons licence, unless indicated otherwise in a credit line to the material. If material is not included in the article's Creative Commons licence and your intended use is not permitted by statutory regulation or exceeds the permitted use, you will need to obtain permission directly from the copyright holder. To view a copy of this licence, visit <http://creativecommons.org/licenses/by-nc-nd/4.0/>.

Background

Tooth extraction and the progressive pneumatization of the maxillary sinus (MS) can cause difficulties for dental implant replacements in the upper posterior region. Maxillary sinus floor elevation (SFE) is widely used to achieve adequate bone height for implant placement in the posterior maxilla and is considered one of the most predictable bone augmentation procedures currently employed [1, 2].

Although the success rate of SFE procedures has been proven to be high, various complications have been reported both during surgery and in the postoperative period. Sinus membrane perforation (SMP) is the most common intraoperative complication during SFE, and it can result in the loss of graft materials, acute or chronic maxillary sinusitis, and potential implant failure; therefore, maintaining the integrity of the sinus membrane is crucial for achieving short- and long-term success [3, 4].

Addressing how to reduce the graft material absorption and increase the formation of vital new bone has always been a popular topic in research on SFE procedures [5, 6]. Some researchers have studied the characteristics and proportions of graft materials [7, 8], while others have focused on the osteogenic properties of the sinus cavity [9–11]. Although a few studies reported that the sinus membrane may present osteoinductive potential, most studies emphasize the importance of maximizing contact between the graft material and sinus wall to promote bone healing. This approach is important, as sinus walls serve as the major source of osteoprogenitor cells and blood supply [10, 11].

The morphology of MS can either facilitate or complicate the incidence of Schneiderian membrane perforation (SMP), as well as the reconstruction of the graft material. Therefore, the existing sinus anatomic variations are factors that should be considered in preliminary surgical decision making. To the best of the authors' knowledge, there remains no standard way to classify sinus contours. Contemporary studies proposing MS contour classification systems mainly focus on a single cone beam measurement Sects. [12–14], despite the MS being stereoscopic and irregular, with different buccal-palatal and mesial-distal contours. Describing the entire MS based on a single section has limitations that can easily lead to an incorrect preoperative diagnosis.

Due to its low level of radiation exposure and higher diagnostic capability, cone beam computed tomography (CBCT) has become an essential diagnostic tool with many applications in implant dentistry in terms of bone quality and MS assessment, as well as in surgery itself [15, 16]. For this reason, we propose a comprehensive MS contour classification system based on a review of the literature and analysis of the characteristics of different groups determined through CBCT examination. We

then discuss the relationship between sinus contours and SFE, aiming to help surgeons improve their presurgical evaluations.

Materials and methods

Study design

The study was approved by the Ethics Committee of the Stomatological Hospital of Southern Medical University (approval number [2022] 08). Written informed consent was obtained from all participants. The CBCT scans were obtained from patients who required dental implant rehabilitation attending the Implantology Center at the Stomatological Hospital affiliated with Southern Medical University, China, between June 2017 and December 2023. The inclusion criteria were: (1) patients were older than 18 years old; (2) patients had single tooth loss in the posterior maxilla with a healing period of more than 12 weeks; and (3) patients had a residual bone height (RBH) of less than 10 mm. The exclusion criteria were: (1) images that were unclear or incomplete; (2) the presence of sinus pathology that made measurement impossible; (3) the absence of adjacent or opposing teeth such that the location of the edentulous ridges corresponding to the tooth site could not be identified; and (4) the presence of previous sinus grafts or implants.

Image acquisition

Radiographic examination was performed with a Newton CBCT (Quantitative Radiology, Verona, Italy). Patients were positioned parallel to the floor with reference to the Frankfort horizontal plane. The technical parameters were set as follows: anode voltage, 110 kV; anode current, 3 to 4.5 mA; scan time, 18 s; field of view (FOV), 12 cm × 15 cm; and voxel size, 200 μm. Multi-planar reconstructions were viewed using the CBCT imaging modality with the instrument's self-contained software program (ImageViewer, Guangzhou, China).

Sample size calculation

A priori power analysis was carried out during the study planning stage to determine an appropriate sample size for robust statistical analysis. To detect differences between the two groups with a two-sided 5% significance level and a power of 80%, at least of 275 tooth sites were deemed necessary.

Data collection

Qualified scans were reoriented to ensure bilateral symmetry of the maxilla and alignment of the hard palate parallel to the ground. A reference arch (80 mm wide) was drawn at the level of the crestal bone on cross-sectional views, with its center corresponding to the center of the ridge. The sinus contours were read using coronal and sagittal images obtained at specific areas

corresponding to the first premolar, second premolar, and molar sites (PM1, PM2, M1, M2). As part of the qualitative research approach, two general practitioners (Lin and Zheng) reconstructed and observed the images. Inter-examiner variability was measured during the study with CBCT scans, where 20 randomly selected patient scans were reviewed by both practitioners (kappa=0.65 to 0.8, indicating moderate to good consistency). Afterwards, one of the reviewers (Lin) took the remaining measurements and recordings of the MS.

MS classification

The comprehensive MS classification proposed in this study is based on previous studies published by Niu [12] and French [13]. In terms of coronal sections, the MS was divided into five subgroups: Type A=narrow tapered; Type B=taper; Type C=ovoid; Type D=square; and Type E=irregular (convex or septa in MS floor). For sagittal sections, MS contour was divided into four subgroups: Type 1=flat; Type 2=slope; Type 3=concave, Type 4=irregular (septa in MS floor). A total of 13 theoretical MS morphologies were thus categorized based on combinations of the classifications mentioned above (Fig. 1): A1: Type A and Type 1; A2: Type A and Type 2; A3: Type A and Type 3; B1: Type B and Type 1; B2: Type

B and Type 2; B3: Type B and Type 3; C1: Type C and Type 1; C2: Type C and Type 2; C3: Type C and Type 3; D1: Type D and Type 1; D2: Type D and Type 2; D3: Type D and Type 3; E: Type E or Type 4. The MS was classified at each tooth position based on the specific morphology observed at that site.

MS characteristics

The following anatomical structures and variations were assessed at the coronal section: (1) residual bone height (RBH): the distance from the most coronal point of the alveolar crest and the MS floor; (2) maxillary sinus angle (MSA): the angle formed at the floor of the MS by a tangent along the buccal and palatal bone walls of the MS. To measure MSA, two horizontal line was drawn at 3 mm and 10 mm from the sinus floor [17]. (Fig. 2A); (3) buccal dip angle (BDA): the angle between the buccal bone plate and the horizontal plane (Fig. 2A); (4) sinus width (SW): the distance between the buccal and palatal walls at 3 mm, 5 mm, 7 mm, and 9 mm from the sinus floor (Fig. 2B); (5) palatonasal recess (PNR): the angle between the lateral nasal wall and the palatal wall within the MS [18] (Fig. 3A), and risk PNR: the PNR located <15 mm from the alveolar crest, with an angle of <90°; both the location of the PNR and its angulation were measured;

	A1	B1	C1	D1	
Buccal-palatal contour					
Mesial-distal contour					
	A2	B2	C2	D2	
Buccal-palatal contour					
Mesial-distal contour					
	A3	B3	C3	D3	E
Buccal-palatal contour					
Mesial-distal contour					

Fig. 1 Comprehensive sinus contour classification

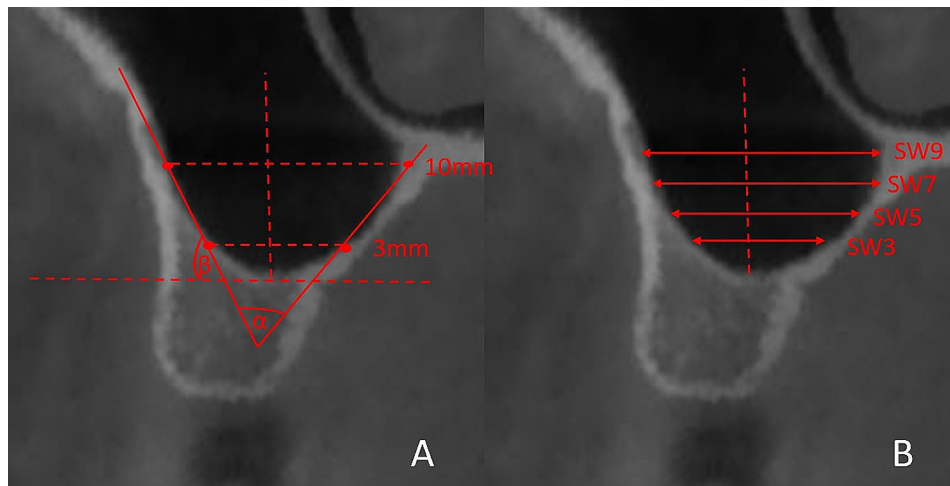


Fig. 2 Sinus characteristics. (A) Angle α : maxillary sinus angle (MSA), Angle β : buccal dip angle (BDA). (B) Sinus width (SW) at 3 mm, 5 mm, 7 mm, and 9 mm from the sinus floor

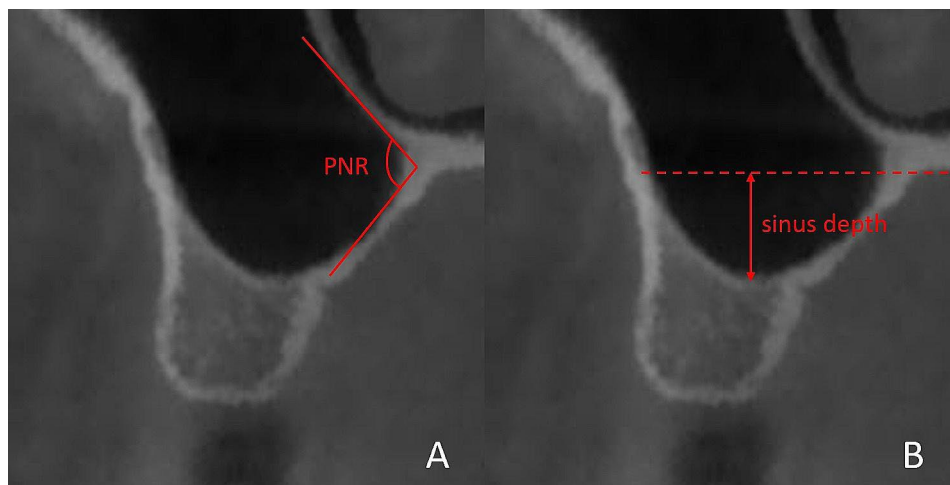


Fig. 3 Sinus characteristics. (A) Palatonasal recess (PNR). (B) sinus depth (type II)

and (6) sinus depth: sinuses were divided according to their extension into the alveolar process as measured from the hard palate: either above (I), 0 to 6 mm below (II), or more than 6 mm below (III) (Fig. 3B) [19].

Statistical analysis

The statistical analysis was performed using SPSS 22.0 (IBM Corp., Armonk, USA). Qualitative data were displayed as mean values and standard deviations. For quantitative variables, frequency was determined. The normal distribution and variance homogeneity were measured. Normally distributed data with homogeneity of variance were analyzed using one-way analysis of variance (ANOVA). Non-normally distributed data were analyzed using the Welch test. The Pearson correlation coefficient (r) was used to test the correlations between variables, with an r value approaching +1 indicating a stronger positive correlation and one approaching -1 indicating

a stronger negative correlation. Statistical difference was determined at $p < 0.05$.

Results

Patients

A total of 266 patients (150 female and 116 male) with 283 tooth sites were included in the study, as 17 patients had unilateral edentulism in the MS. The mean age of the patients was 40.0 ± 14.7 years. The included number of PM1s, PM2s, M1s, and M2s was 18, 60, 142, and 63, respectively.

Characteristics of different MS contours

MS contours were categorized into 11 groups, as no A1 and A3 patients remained in the sample after detailed calculations. Statistical analysis revealed significant differences among the different groups, including in RBH, MSA, and BDA, as illustrated in Table 1.

Table 1 Characteristics of different MS contours, mean (±SD)

	RBH(mm)	BDA(°)	MSA(°)
A2	8.66(0.77)	79.90(3.18)	19.89(8.01)
B1	6.70(1.91)	60.83(10.34)	48.27(7.72)
B2	6.81(1.52)	65.27(13.54)	49.05(8.11)
B3	5.41(2.41)	62.87(13.85)	50.82(8.35)
C1	6.99(2.06)	53.04(9.26)	70.13(9.59)
C2	6.69(1.37)	56.40(10.57)	71.33(7.82)
C3	5.27(2.04)	50.65(8.78)	74.66(11.52)
D1	5.93(2.10)	50.78(13.01)	65.62(18.28)
D2	7.98(2.00)	56.34(6.61)	54.73(27.39)
D3	5.11(2.70)	52.49(8.14)	64.69(11.64)
E	6.79(1.70)	56.13(13.48)	61.57(16.77)
Mean	6.37(2.09)	57.11(12.89)	60.94(16.97)
F value	9.648	9.282	45.949
P value	0.000	0.000	0.000

RBH: residual bone height; BDA: buccal dip angle; MSA: maxillary sinus angle

RBH

The A2 and D2 groups had the most sufficient RBH, with an average height of approximately 8 mm. In comparison, the average RBH for the B3, C3, D1, and D3 groups was less than 6 mm. RBH was weakly negatively correlated with SW9 ($r = -0.232, P < 0.05$).

MSA

The sharpest average MSA was less than 20° and observed in the A2 group. The mean MSA of the C groups was larger than 70°, and the largest angle was in the C3 group.

BDA

Contrary to that of the MSA, the largest average BDA was in the A2 group at approximately 80°. The smallest BDA was in the C3 group. The correlation coefficient between BDA and MSA was $-0.625 (P < 0.05)$, indicating a strongly negative correlation.

SW

Overall, SW became wider at higher measurement levels except for the SW in the A2 group (Fig. 4). The D1 and D3 groups had the widest SW at all measurement levels, which was two times wider at SW3 and three times wider at SW9 than those of the A2 group. SW9 was strongly positively correlated with MSA ($r = 0.67, P < 0.05$) and strongly negatively correlated with BDA ($r = -0.65, P < 0.05$).

PNR

PNR was identified in 38% of CBCT scans. Mean PNR was $104.06 \pm 16.83^\circ$ and the mean height was 14.72 ± 11.78 mm from the alveolar crest. The highest prevalence of PNR was 63.8% in the C2 group. The

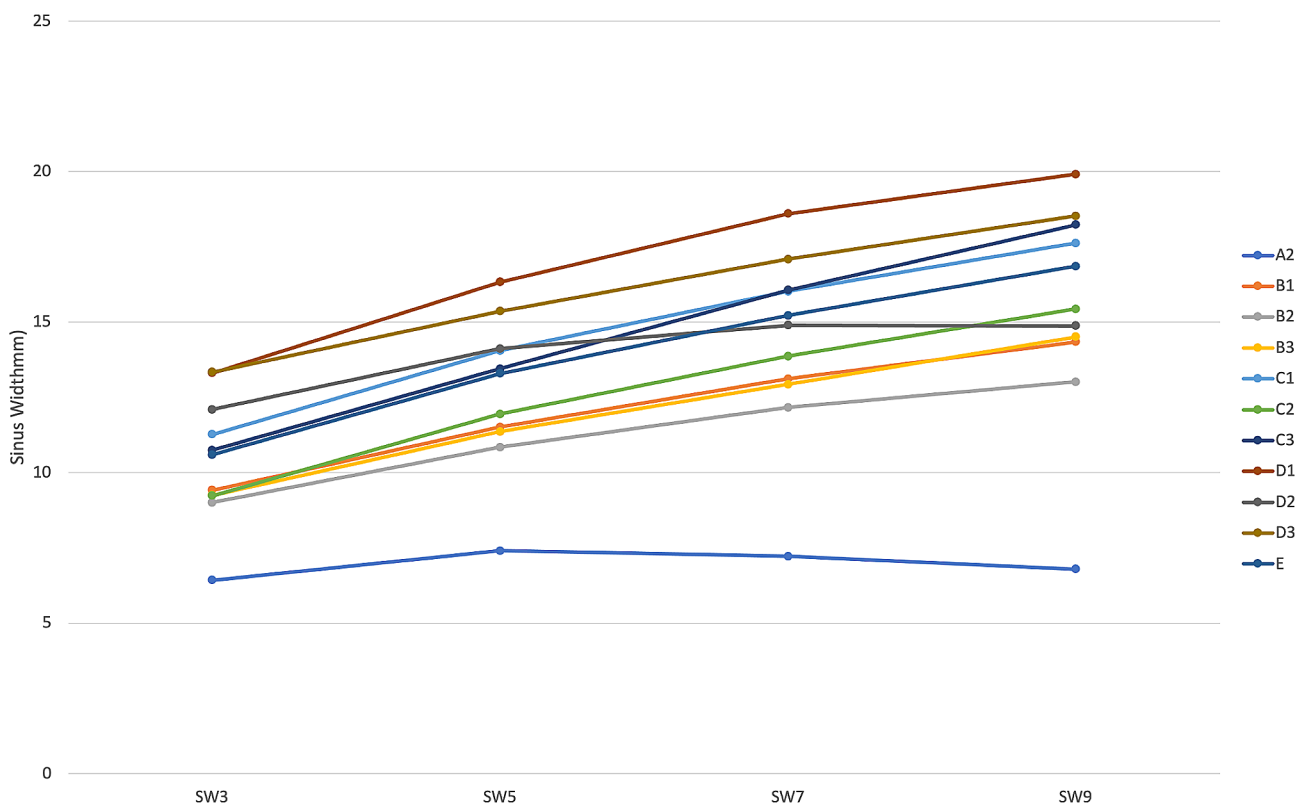


Fig. 4 Sinus width (SW) variation among different groups and measurement levels

average angle of risk PNR, which was observed in 11.7% of CBCT scans, was $86.11 \pm 5.91^\circ$, and the average height was 12.49 ± 2.03 mm. Regarding distribution, 60% of the D3 PNRs were at risk sites. No risk of PNR was found in the A2, C1, or D1 groups.

Sinus depth

The overall percentage of Type I, II, and III sinus was 17.1% (48/283), 53.4% (151/283), and 29.2% (84/283), respectively. The distribution of the D1 group was most uneven, with 80% of WS categorized as Type II. Nearly 45% of the C3 and D3 groups were categorized as Type III sinus, compared with 20 to 30% of the other groups.

Distribution of different MS contours

The distribution of different MS contours is illustrated in Table 2. The MS contours were dispersed among different tooth sites, with no classification accounting for more than 35% at one tooth site. The B2 and B3 groups were more often observed in PM1 (22.2%, 4/18). The B2 group comprised the largest proportion of the PM2 area (28.3%, 17/60). In the M1 area, C3 group was the most common morphology (30.9%, 44/142). In the M2 area, B1 group was the most common morphology (25.3%, 16/63). The E groups comprised 15.9% (45/283) of the total MS classification.

Discussion

The present study revealed significant variations in MS among different measurement sections and tooth positions, preventing the development of a simple and meaningful classification of the entire sinus and one measurement section.

Characteristics of different MS contours

Relationship between RBH and sinus depth

RBH is a key factor in determining the surgical approach for SFE. The Academy of Osseointegration Consensus

Conference on Sinus Grafts recommends transcristal SFE with simultaneous implant placement for RBH larger than 6 mm; lateral SFE for RBH 6 mm or smaller; and, in particular, lateral SFE with staged implant placement when RBH is smaller than 4 mm [20]. Several studies have proposed that as the impact of RBH does not appear to affect osteogenesis, greater emphasis should be placed on SFE surgical difficulty and complications [21, 22]. The results of the present study suggest that RBH is more strongly determined by the mesial-distal sinus contour with a trend toward a sloping>flat>concave site. This suggestion is partially in line with French et al. [13], whose study of single and multiple tooth loss revealed that RBH was highest in sloping MS, followed by concave and flat MS. Such findings demonstrate the morphology variation between single and multiple tooth loss. In areas of multiple tooth loss, the sinus floor becomes flatter due to the extensive pneumatization and absence of support from adjacent teeth. Comparatively, the sinus floor tends to present a concave morphology in an area of single tooth loss because pneumatization is localized [13, 23, 24]. Several studies have also indicated that when the tooth root protrudes into the MS, the sinus floor often exhibits a deep concave morphology and low RBH after tooth extraction [24, 25]. Such a phenomenon may well explain our results.

The findings of the present study concur with those of Wagner et al., who found that RBH gradually decreases with increasing sinus depth [19]. This can be attributed to the greater extension of the MS into the alveolar process, inevitably resulting in a reduction of the RBH. Teng et al. [26]. and Berl et al. [27]. found a negative correlation between RBH and SW, as did the present study, albeit only a weakly negative correlation. All these results suggest that RBH is more influenced by the vertical pneumatization of the MS rather than the horizontal direction.

SW characteristics

Several studies classified MS into narrow, medium, or wide on the basis of SW [14, 26]. Nonetheless, our findings indicate that SW varies with measurement height and tooth position, rendering a classification based solely on this parameter impractical. In Bertl et al.'s observational study [27], dimensional differences in SW among different tooth sites at lower measurement levels were minimal. By contrast, our research identified significant SW variations in relation to MS contours. The SW was maintained at a similar dimension in the A2 group and became even narrower at SW7 and SW9, possibly because the middle third of the nasal cavity was larger at these measurement levels. Except for the A2 group, all the groups exhibited an increase in SW at higher measurement levels, with SW tending to increase from

Table 2 Distribution of different MS contours, n (%)

	PM1	PM2	M1	M2	Total
A2	3	5	1	1	10 (3.5)
B1	2	3	7	16	27 (9.5)
B2	4	17	5	9	35 (12.4)
B3	4	2	14	5	27 (9.5)
C1	0	4	22	13	38 (13.4)
C2	2	4	4	1	11 (3.9)
C3	1	3	44	2	51 (18)
D1	0	5	11	5	21 (7.4)
D2	0	6	0	1	7 (2.5)
D3	0	0	11	0	11 (3.9)
E	2	11	22	10	45 (15.9)
Total	18	60	142	63	283

PM1: first premolar; PM2: second premolar; M1: first molar; M2: second molar

narrow-taper to irregular type, a result in alignment with the findings of Niu et al. [12].

Relationship between MSA and BDA

First proposed by Cho et al. [17], the MSA is a parameter describing the axial angle between the buccal and palatal bony walls. Since then, the MSA has been measured by different methods in different studies [28, 29]. We selected Cho et al.'s method, which is considered the traditional measurement method. Clinicians have frequently investigated the relationship between the MSA and SMP [17, 29–31]. In their study, Cho et al. [17], observed that when the MSA was smaller than 30°, the SMP rate was 37.5% and decreased to 28.6% and 0% when the MSA was from 30° to 60° and greater than 60°, respectively. Pizzini et al. found that when the MSA was smaller than 90°, the SMP rate was the highest at 38%, and the rate was twice as high when the MSA was greater than 90° [29]. All these studies provide evidence that sharper MSA is associated with higher SMP probability.

Although the MSA reflects the entire MS floor morphology on coronal sections, it cannot describe the morphology of the buccal and palatal bony walls individually. To address this problem, Pi et al. first introduced dip angle as a means of classifying the sinus contour [32]. To the best of our knowledge, our study was the first study investigating the characteristics of the buccal dip angle from radiographic examinations in a large sample of patients. Our findings revealed a strongly negative correlation between SW and BDA, indicating that an increased buccal inclination of the bony wall corresponds to a wider MS. We attempted but failed to measure the palatal dip angle because of the difficulty of measuring it objectively due to the irregular morphology of the nasal cavity and the existence of the PNR. Although the C groups had the most buccal inclined bony wall, the D groups had the widest SW. These findings provide evidence that the palatal bony wall of the square sinus is significantly more tilted toward the nasal cavity than the other morphology of the MS.

PNR

The PNR is an anatomical structure between the roof of the hard palate and the lateral wall of the nasal cavity [18]. In our series, the highest prevalence of PNR was sloping MS, followed by concave and flat MS. Wagner et al., who first identified PNR, proposed that sharp-angled recesses (<90°) might hinder sinus membrane elevation on the palatal wall [12, 18, 33]. Interestingly, we observed that concave sinus posed a greater risk of PNR than the sloping sites. Specifically, more than 50% of the C3 and D3 groups, which have the lowest RBH and widest SW, exhibited PNR at risk sites.

Distribution of different MS contours

The anterior border of the MS usually starts from the mesial or distal apex of the PM1 and PM2, commonly leading to a sloping sinus floor in the anterior part of the MS. At the same time, most concave sites are between adjacent teeth or septa, and therefore the concave contour is most frequently observed in the M1 from the sagittal section. As pneumatization is more sufficient in the coronal section in the middle part of the MS, ovoid and square shapes are often seen in the M1, followed by a taper shape in the PM2 and M2 and a narrow-taper shape in the PM1 [34]. Despite the existence of certain characteristics at different tooth sites, diverse classification systems have been used within the same tooth position, indicating large anatomical variations in the MS.

The prevalence of irregular MS in the current study was 15.9%, slightly lower than that reported in other studies [35, 36]. This variance could be attributed to our measurement at individual tooth sites rather than the measure of the entire sinus. In addition, we did not classify transverse septa located in the upper third of the MS into the E group because we did not observe them on the sinus floor.

Characteristics of extensive pneumatization MS

Using the classification system proposed by Kalavagunta et al. [37], we found that the prevalence of extensive pneumatization in our study was 8.1%. The morphological characteristics of extensive pneumatization were consistent, including (1) a deep concave sinus floor (78.2%); (2) an extremely low RBH, typically smaller than 3 mm (69.5%); (3) a thin buccal and palatal bony wall, typically thinner than 1 mm (100%); (4) a sharp angled PNR (86.9%); and (5) an unobservable sinus membrane on CBCT scans (100%).

Application of comprehensive MS contour classification

Based on comprehensive MS contour classification and analysis of the characteristics observed on radiographic examination, we present several clinical recommendations based on the reviewed literature and the expertise of the authors.

1. The E group (irregular sinus) presents the most significant surgical challenges during SFE and leads to the highest percentage of SMP. Transcrestal SFE may not be a good option for this morphology because it requires a higher mallet force to elevate the sinus membrane, and an inadequate force may possibly cause SMP. Several methods have been introduced to manage the presence of septa, including those based on avoidance of sinus septa; use of a surgical method that comprises the formation of several trap windows, depending

- on the height of the septa; and methods based on the simultaneous removal of septa [12, 13, 38–40]. Utilizing digital guides can enhance the precise positioning of the surgical window, thereby improving surgical accuracy and safety [40, 41].
2. The A2 group (narrow and slope sinus) also has a high risk of SMP. Fortunately, SFE is usually avoidable or does not require much vertical elevation, as the average RBH was more than 8 mm in this group. When SFE is unavoidable, a modified lateral SFE with an inferior margin of the window at the same level as the sinus floor might be indicated [12].
 3. The incidence of SMP is lower in cases where a taper or slope sinus floor is identified on CBCT scans. Both transcresal and lateral SFE techniques are advisable. It is noteworthy that the force applied from the osteotome is uneven in the slope sinus, and uneven tension during detachment of the mucosa is assumed to be responsible for SMP. Moreover, to elevate the sinus membrane sufficiently, the lower site of the angle sinus usually requires a greater elevation height, which increases the possibility of SMP. We recommend employing minimally invasive surgical tools to minimize the risk of SMP [42, 43]. Graftless SFE could also be a reliable approach to reduce augmentation procedures in patients, particularly when SMP occurs, thereby minimizing the need for graft material replacement into the sinus [44, 45].
 4. SMP possibility was lowest when the contour was ovoid or square in the coronal section and concave or flat in the sagittal section. However, these groups usually had a lower RBH and wider SW. It is difficult to elevate the sinus membrane by osteotome thoroughly in wider MS, posing the risk of partial or complete embedding of the graft material beneath the sinus membrane. This impedes the infiltration of blood supply and osteogenic factors from the bony walls into the graft, resulting in increased graft resorption and reduced formation of vital new bone [22, 28, 46]. Although transcresal SFE might be considered in cases with low RBH, lateral SFE is preferred for MS with a larger SW. Clinicians are advised to increase the proportion of autogenous bone and extend the healing period for better outcomes.

This study has several limitations that should be considered when reviewing the findings. First, it remains unclear whether the absence of the A1 and A3 groups was due to the study design or limitations in the dataset; this requires further validation with larger sample sizes. Second, several of the 11 groups examined in this study

included fewer patients than the other groups, potentially introducing bias into the statistical analysis. Third, a considerably smaller sample was examined at premolar sites, especially the PM1 area, and the timing of the process of becoming edentulous was not documented. Given these limitations, the findings of this study may have more implications for molar sites. Finally, most published studies have described the MS characteristics based on different tooth positions; however, studies that describe MS characteristics based on sinus contour classification are lacking. The limitations of currently published studies hinder direct comparisons between our study and others, as the grouping methods vary. Despite this, we have verified the rationality of our data based on different tooth positions, and our results show numerical consistency with the clinically published literature.

Conclusion

Anatomical variations in the MS underscore the importance of specific treatment approaches and customized SFE planning. Thus, performing CBCT routinely prior to surgery is stressed. Despite distinct characteristics observed among different tooth sites, diverse classifications were found within the same tooth position, indicating large anatomical variability in the MS. The classification provided herein outlines generalized characteristics specific to individual tooth sites, aiming to help surgeons perform better presurgical evaluations.

Abbreviations

MS	Maxillary sinus
SFE	Sinus floor elevation
CBCT	Cone beam computed tomography
SMP	Sinus membrane perforation
RBH	Residual bone height
MSA	Maxillary sinus angle
BDA	Buccal dip angle
SW	Sinus width
PNR	Palatonasal recess

Acknowledgements

We thank LetPub (www.letpub.com) for its linguistic assistance during the preparation of this manuscript.

Author contributions

Lin X and Que G developed the concept and design of this study. Lin X, Li SB, Zheng X performed the clinical examination and contributed to the analysis of behavioral data. Lin X performed statistical analyses, and all authors contributed to the interpretation of the data. Lin X drafted the manuscript. All authors read and approved the final manuscript.

Funding

Study supported in part by Research and Cultivation Project of Stomatological Hospital, Southern Medical University (Grant Number: PY2023032), and Science and Technology Project of Guangzhou City (Grant Number: 201903010038).

Data availability

Due to the data herein was part of the content of the first author's PHD dissertation (not published), the datasets generated during the current study are not publicly available but are available from the corresponding author on reasonable request.

Declarations

Ethics approval and consent to participate

The study was approved by Ethics Committee of the Stomatological Hospital of Southern Medical University (approval number [2022] 08).

Consent for publication

Not applicable.

Competing interests

The authors declare no competing interests.

Received: 20 March 2024 / Accepted: 5 August 2024

Published online: 30 August 2024

References

- Shah D, Chauhan C, Shah R. Survival rate of dental implant placed using various maxillary sinus floor elevation techniques: a systematic review and meta-analysis. *J Indian Prosthodont Soc.* 2022 2022;22(3):215–24. http://www.ncbi.nlm.nih.gov/entrez/query.fcgi?cmd=Retrieve&db=pubmed&dopt=Abstract&list_uids=36511050&query_hl=1https://doi.org/10.4103/jips.jips_283_22
- Raghoobar GM, Onclin P, Boven GC, Vissink A, Meijer H. Long-term effectiveness of maxillary sinus floor augmentation: a systematic review and meta-analysis. *J Clin Periodontol.* 2019 2019;46 Suppl 21:307–18. http://www.ncbi.nlm.nih.gov/entrez/query.fcgi?cmd=Retrieve&db=pubmed&dopt=Abstract&list_uids=30624789&query_hl=1https://doi.org/10.1111/jcpe.13055
- Kim JS, Choi SM, Yoon JH, Lee EJ, Yoon J, Kwon SH et al. What affects post-operative sinusitis and implant failure after dental implant: a meta-analysis. *Otolaryngol Head Neck Surg.* 2019. 2019;160(6):974–84. http://www.ncbi.nlm.nih.gov/entrez/query.fcgi?cmd=Retrieve&db=pubmed&dopt=Abstract&list_uids=30776960&query_hl=1https://doi.org/10.1177/0194599819829747
- Al-Moraissi E, Elsharkawy A, Abotaleb B, Alkebsi K, Al-Motwakel H. Does intraoperative perforation of schneiderian membrane during sinus lift surgery causes an increased the risk of implants failure? A systematic review and meta regression analysis. *Clin Implant Dent Relat Res.* 2018. 2018;20(5):882–89. http://www.ncbi.nlm.nih.gov/entrez/query.fcgi?cmd=Retrieve&db=pubmed&dopt=Abstract&list_uids=30168884&query_hl=1https://doi.org/10.1111/cid.12660
- Al-Moraissi E, Alhaji WA, Al-Qadhi G, Christidis N. Bone graft osseous changes after maxillary sinus floor augmentation: a systematic review. *J Oral Implantol.* 2022 2022;48(5):464–71. http://www.ncbi.nlm.nih.gov/entrez/query.fcgi?cmd=Retrieve&db=pubmed&dopt=Abstract&list_uids=35881815&query_hl=1https://doi.org/10.1563/aaid-joi-D-21-00310
- Coopman R, Fennis J, Ghaemina H, Van de Vyvere G, Politis C, Hoppenreijts T. Volumetric osseous changes in the completely edentulous maxilla after sinus grafting and lateral bone augmentation: a systematic review. *Int J Oral Maxillofac Surg.* 2020 2020;49(11):1470–80. http://www.ncbi.nlm.nih.gov/entrez/query.fcgi?cmd=Retrieve&db=pubmed&dopt=Abstract&list_uids=32241580&query_hl=1https://doi.org/10.1016/j.ijom.2020.03.001
- Canelas J, Drugos L, Ritto FG, Fischer RG, Medeiros P. Xenograft materials in maxillary sinus floor elevation surgery: a systematic review with network meta-analyses. *Br J Oral Maxillofac Surg.* 2021 2021;59(7):742–51. http://www.ncbi.nlm.nih.gov/entrez/query.fcgi?cmd=Retrieve&db=pubmed&dopt=Abstract&list_uids=34120778&query_hl=1https://doi.org/10.1016/j.bjoms.2021.02.009
- Li X, Lin SC, Duan SY. The impact of deproteinized bovine bone particle size on histological outcomes in sinus floor elevation: a systematic review and meta-analysis. *Int J Implant Dent.* 2023 2023;9(1):35. http://www.ncbi.nlm.nih.gov/entrez/query.fcgi?cmd=Retrieve&db=pubmed&dopt=Abstract&list_uids=37782429&query_hl=1https://doi.org/10.1186/s40729-023-00502-1
- Lie N, Merten HA, Meyns J, Lethaus B, Wiltfang J, Kessler P. Elevation of the maxillary sinus membrane for de-novo bone formation: first results of a prospective study in humans. *J Craniomaxillofac Surg.* 2015 2015;43(8):1670–77. http://www.ncbi.nlm.nih.gov/entrez/query.fcgi?cmd=Retrieve&db=pubmed&dopt=Abstract&list_uids=26293185&query_hl=1https://doi.org/10.1016/j.jcms.2015.07.011
- Scala A, Botticelli D, Faeda RS, Garcia RIJ, Americo DOJ, Lang NP. Lack of influence of the schneiderian membrane in forming new bone apical to implants simultaneously installed with sinus floor elevation: an experimental study in monkeys. *Clin Oral Implants Res.* 2012. 2012;23(2):175–81. http://www.ncbi.nlm.nih.gov/entrez/query.fcgi?cmd=Retrieve&db=pubmed&dopt=Abstract&list_uids=21668505&query_hl=1https://doi.org/10.1111/j.1600-0501.2011.02227.x
- Jungner M, Cricchio G, Salata LA, Sennerby L, Lundqvist C, Hultcrantz M et al. On the early mechanisms of bone formation after maxillary sinus membrane elevation: an experimental histological and immunohistochemical study. *Clin Implant Dent Relat Res.* 2015 2015;17(6):1092–102. http://www.ncbi.nlm.nih.gov/entrez/query.fcgi?cmd=Retrieve&db=pubmed&dopt=Abstract&list_uids=24629171&query_hl=1https://doi.org/10.1111/cid.12218
- Niu L, Wang J, Yu H, Qiu L. New classification of maxillary sinus contours and its relation to sinus floor elevation surgery. *Clin Implant Dent Relat Res.* 2018. 2018;20(4):493–500. http://www.ncbi.nlm.nih.gov/entrez/query.fcgi?cmd=Retrieve&db=pubmed&dopt=Abstract&list_uids=29691967&query_hl=1https://doi.org/10.1111/cid.12606
- French D, Nadji N, Liu SX, Larjava H. Trifactorial classification system for osteotome sinus floor elevation based on an observational retrospective analysis of 926 implants followed up to 10 years. *Quintessence Int.* 2015 2015;46(6):523–30. http://www.ncbi.nlm.nih.gov/entrez/query.fcgi?cmd=Retrieve&db=pubmed&dopt=Abstract&list_uids=25918758&query_hl=1https://doi.org/10.3290/j.qia.33935
- Chan HL, Suarez F, Monje A, Benavides E, Wang HL. Evaluation of maxillary sinus width on cone-beam computed tomography for sinus augmentation and new sinus classification based on sinus width. *Clin Oral Implants Res.* 2014. 2014;25(6):647–52. http://www.ncbi.nlm.nih.gov/entrez/query.fcgi?cmd=Retrieve&db=pubmed&dopt=Abstract&list_uids=23043676&query_hl=1https://doi.org/10.1111/clr.12055
- Lozano-Carrascal N, Salomo-Coll O, Gehrke SA, Calvo-Guirado JL, Hernandez-Alfaro F, Gargallo-Albiol J. Radiological evaluation of maxillary sinus anatomy: a cross-sectional study of 300 patients. *Ann Anat.* 2017 2017;214:1–08. http://www.ncbi.nlm.nih.gov/entrez/query.fcgi?cmd=Retrieve&db=pubmed&dopt=Abstract&list_uids=28759740&query_hl=1https://doi.org/10.1016/j.aanat.2017.06.002
- Zeng P, Song R, Lin Y, Li H, Chen S, Shi M et al. Abnormal maxillary sinus diagnosing on cbct images via object detection and 'straight-forward' classification deep learning strategy. *J Oral Rehabil.* 2023. 2023;50(12):1465–80. http://www.ncbi.nlm.nih.gov/entrez/query.fcgi?cmd=Retrieve&db=pubmed&dopt=Abstract&list_uids=37665121&query_hl=1https://doi.org/10.1111/joor.13585
- Cho SC, Wallace SS, Froum SJ, Tarnow DP. Influence of anatomy on schneiderian membrane perforations during sinus elevation surgery: three-dimensional analysis. *Pract Proced Aesthet Dent.* 2001 2001;13(2):160–63. http://www.ncbi.nlm.nih.gov/entrez/query.fcgi?cmd=Retrieve&db=pubmed&dopt=Abstract&list_uids=11315435&query_hl=1
- Chan HL, Monje A, Suarez F, Benavides E, Wang HL. Palatonasal recess on medial wall of the maxillary sinus and clinical implications for sinus augmentation via lateral window approach. *J Periodontol.* 2013 2013;84(8):1087–93. http://www.ncbi.nlm.nih.gov/entrez/query.fcgi?cmd=Retrieve&db=pubmed&dopt=Abstract&list_uids=23106503&query_hl=1https://doi.org/10.1902/jop.2012.120371
- Wagner F, Dvorak G, Nemes S, Pietschmann P, Traxler H, Schicho K et al. Morphometric analysis of sinus depth in the posterior maxilla and proposal of a novel classification. *Sci Rep.* 2017. 2017;7:45397. http://www.ncbi.nlm.nih.gov/entrez/query.fcgi?cmd=Retrieve&db=pubmed&dopt=Abstract&list_uids=28338085&query_hl=1https://doi.org/10.1038/srep45397
- Jensen OT, Shulman LB, Block MS, Iacono VJ. Report of the sinus consensus conference of 1996. *Int J Oral Maxillofac Implants.* 1998 1998;13 Suppl:11–45. http://www.ncbi.nlm.nih.gov/entrez/query.fcgi?cmd=Retrieve&db=pubmed&dopt=Abstract&list_uids=9715571&query_hl=1
- Pignatton TB, Wenzel A, Ferreira C, Borges MC, Oliveira G, Marcantonio EJ et al. Influence of residual bone height and sinus width on the outcome of maxillary sinus bone augmentation using anorganic bovine bone. *Clin Oral Implants Res.* 2019. 2019;30(4):315–23. http://www.ncbi.nlm.nih.gov/entrez/query.fcgi?cmd=Retrieve&db=pubmed&dopt=Abstract&list_uids=30803035&query_hl=1https://doi.org/10.1111/clr.13417
- Zhou W, Wang F, Magic M, Zhuang M, Sun J, Wu Y. The effect of anatomy on osteogenesis after maxillary sinus floor augmentation: a radiographic and histological analysis. *Clin Oral Investig.* 2021 2021;25(9):5197–204. http://www.ncbi.nlm.nih.gov/entrez/query.fcgi?cmd=Retrieve&db=pubmed&dopt=Abstract&list_uids=33569678&query_hl=1https://doi.org/10.1007/s00784-021-03827-6
- Dursun E, Keceli HG, Dolgun A, Velasco-Torres M, Olculer M, Ghoreishi R et al. Maxillary sinus and surrounding bone anatomy with cone beam computed

- tomography after multiple teeth loss: a retrospective multicenter clinical study. *Implant Dent.* 2019 2019;28(3):226–36. http://www.ncbi.nlm.nih.gov/entrez/query.fcgi?cmd=Retrieve&db=pubmed&dopt=Abstract&list_uids=31124819&query_hl=1https://doi.org/10.1097/ID.0000000000000862
24. Cavalcanti MC, Guirado TE, Sapata VM, Costa C, Pannuti CM, Jung RE, et al. Maxillary sinus floor pneumatization and alveolar ridge resorption after tooth loss: a cross-sectional study. *Braz Oral Res.* 2018 2018 Aug 6;32:e64. Available from: http://www.ncbi.nlm.nih.gov/entrez/query.fcgi?cmd=Retrieve&db=pubmed&dopt=Abstract&list_uids=3008851&query_hl=1.https://doi.org/10.1590/1807-3107BOR-2018.vol32.0064
 25. Themkumkwun S, Kitisubkanchana J, Waikakul A, Boonsiriseth K. Maxillary molar root protrusion into the maxillary sinus: a comparison of cone beam computed tomography and panoramic findings. *Int J Oral Maxillofac Surg.* 2019 2019;48(12):1570–76. http://www.ncbi.nlm.nih.gov/entrez/query.fcgi?cmd=Retrieve&db=pubmed&dopt=Abstract&list_uids=31235390&query_hl=1https://doi.org/10.1016/j.jiom.2019.06.011
 26. Teng M, Cheng Q, Liao J, Zhang X, Mo A, Liang X. Sinus width analysis and new classification with clinical implications for augmentation. *Clin Implant Dent Relat Res.* 2016. 2016;18(1):89–96. http://www.ncbi.nlm.nih.gov/entrez/query.fcgi?cmd=Retrieve&db=pubmed&dopt=Abstract&list_uids=25041134&query_hl=1https://doi.org/10.1111/cid.12247
 27. Bertl K, Mick RB, Heimesel P, Gahleitner A, Stavropoulos A, Ulm C. Variation in bucco-palatal maxillary sinus width does not permit a meaningful sinus classification. *Clin Oral Implants Res.* 2018. 2018;29(12):1220–29. http://www.ncbi.nlm.nih.gov/entrez/query.fcgi?cmd=Retrieve&db=pubmed&dopt=Abstract&list_uids=30430654&query_hl=1https://doi.org/10.1111/clr.13387
 28. Zheng X, Huang L, Huang S, Mo A, Zhu J. Influence of anatomical factors related to maxillary sinus on outcomes of transcrestal sinus floor elevation. *J Dent Sci.* 2022 2022;17(1):438–43. http://www.ncbi.nlm.nih.gov/entrez/query.fcgi?cmd=Retrieve&db=pubmed&dopt=Abstract&list_uids=35028068&query_hl=1https://doi.org/10.1016/j.jds.2021.07.023
 29. Pizzini A, Basma HS, Li P, Geurs NC, Abou-Arrej RV. The impact of anatomic, patient and surgical factors on membrane perforation during lateral wall sinus floor elevation. *Clin Oral Implants Res.* 2021. 2021;32(3):274–84. http://www.ncbi.nlm.nih.gov/entrez/query.fcgi?cmd=Retrieve&db=pubmed&dopt=Abstract&list_uids=33314302&query_hl=1https://doi.org/10.1111/clr.13698
 30. Marin S, Kirnbauer B, Rugani P, Payer M, Jakse N. Potential risk factors for maxillary sinus membrane perforation and treatment outcome analysis. *Clin Implant Dent Relat Res.* 2019 2019;21(1):66–72. http://www.ncbi.nlm.nih.gov/entrez/query.fcgi?cmd=Retrieve&db=pubmed&dopt=Abstract&list_uids=30475442&query_hl=1https://doi.org/10.1111/cid.12699
 31. Shao Q, Li J, Pu R, Feng Y, Jiang Z, Yang G. Risk factors for sinus membrane perforation during lateral window maxillary sinus floor elevation surgery: a retrospective study. *Clin Implant Dent Relat Res.* 2021. 2021;23(6):812–20. http://www.ncbi.nlm.nih.gov/entrez/query.fcgi?cmd=Retrieve&db=pubmed&dopt=Abstract&list_uids=34750940&query_hl=1https://doi.org/10.1111/cid.13052
 32. Pi X, Chen D, Liu Q, Ren B, Pan H, Su Y. The decision-making principles of sinus floor elevation (part 2). *Chin J Oral Implants.* 2022;27(06):387–92. https://kns.cnki.net/kcms2/article/abstract?v=9w9hjx65dQQhuZbpMBStXCQqF5sLUjjaeUJNwRhrcQ5YbKwFq55uHGixumAyBC1Os_TawhM7Bje6p5qm-5t35ooETyULL2cKRasi8zXy09o4UXsX9cHilbV4dCfeKylOKR_fu_AKFLsjrG9MBiSag=&uniplatform=NZKPT&language=CHS
 33. Testori T, Tavelli L, Yu SH, Scaini R, Darnahal A, Wallace SS et al. Maxillary sinus elevation difficulty score with lateral wall technique. *Int J Oral Maxillofac Implants.* 2020 2020;35(3):631–38. http://www.ncbi.nlm.nih.gov/entrez/query.fcgi?cmd=Retrieve&db=pubmed&dopt=Abstract&list_uids=32406663&query_hl=1https://doi.org/10.11607/jomi.8034
 34. Whyte A, Boeddinghaus R. The maxillary sinus: physiology, development and imaging anatomy. *Dentomaxillofac Radiol.* 2019 2019;48(8):20190205. http://www.ncbi.nlm.nih.gov/entrez/query.fcgi?cmd=Retrieve&db=pubmed&dopt=Abstract&list_uids=31386556&query_hl=1https://doi.org/10.1259/dmfr.20190205
 35. Henriques I, Carames J, Francisco H, Carames G, Hernandez-Alfaro F, Marques D. Prevalence of maxillary sinus septa: systematic review and meta-analysis. *Int J Oral Maxillofac Surg.* 2022 2022;51(6):823–31. http://www.ncbi.nlm.nih.gov/entrez/query.fcgi?cmd=Retrieve&db=pubmed&dopt=Abstract&list_uids=34742634&query_hl=1https://doi.org/10.1016/j.jiom.2021.10.008
 36. Takeda D, Hasegawa T, Saito I, Arimoto S, Akashi M, Komori T. A radiologic evaluation of the incidence and morphology of maxillary sinus septa in Japanese dentate maxillae. *Oral Maxillofac Surg.* 2019 2019;23(2):233–37. http://www.ncbi.nlm.nih.gov/entrez/query.fcgi?cmd=Retrieve&db=pubmed&dopt=Abstract&list_uids=31089896&query_hl=1https://doi.org/10.1007/s10006-019-00773-2
 37. Kalavagunta S, Reddy KT. Extensive maxillary sinus pneumatization. *Rhinology.* 2003 2003;41(2):113–17. http://www.ncbi.nlm.nih.gov/entrez/query.fcgi?cmd=Retrieve&db=pubmed&dopt=Abstract&list_uids=12868378&query_hl=1
 38. Wen SC, Chan HL, Wang HL. Classification and management of antral septa for maxillary sinus augmentation. *Int J Periodontics Restorative D.* 2013 2013;33(4):509–17. http://www.ncbi.nlm.nih.gov/entrez/query.fcgi?cmd=Retrieve&db=pubmed&dopt=Abstract&list_uids=23820711&query_hl=1https://doi.org/10.11607/prd.1609
 39. Teixeira KN, Sakurada MA, Philippi AG, Goncalves T. Use of a stackable surgical guide to improve the accuracy of the lateral wall approach for sinus grafting in the presence of a sinus septum. *Int J Oral Maxillofac Surg.* 2021 2021;50(10):1383–85. http://www.ncbi.nlm.nih.gov/entrez/query.fcgi?cmd=Retrieve&db=pubmed&dopt=Abstract&list_uids=33678490&query_hl=1https://doi.org/10.1016/j.jiom.2021.02.023
 40. Lyu M, Xu D, Zhang X, Yuan Q. Maxillary sinus floor augmentation: a review of current evidence on anatomical factors and a decision tree. *Int J Oral Sci.* 2023 2023;15(1):41. http://www.ncbi.nlm.nih.gov/entrez/query.fcgi?cmd=Retrieve&db=pubmed&dopt=Abstract&list_uids=37714889&query_hl=1https://doi.org/10.1038/s41368-023-00248-x
 41. Wang T, Ye L, Sun Y, Wu Y. Fabricating a surgical template for guiding sinus floor elevation in the maxillary sinus septa with simultaneous implant placement: a dental technique. *J Prosthet Dent.* 2023 2023;129(6):840–43. http://www.ncbi.nlm.nih.gov/entrez/query.fcgi?cmd=Retrieve&db=pubmed&dopt=Abstract&list_uids=34493391&query_hl=1https://doi.org/10.1016/j.prosdent.2021.07.012
 42. Zadrozny L, Wagner L, Rosenbach D. Minimally invasive transcrestal sinus floor elevation procedure in severely atrophic ridge: a case report. *J Oral Implantol.* 2021 2021;47(3):215–22. http://www.ncbi.nlm.nih.gov/entrez/query.fcgi?cmd=Retrieve&db=pubmed&dopt=Abstract&list_uids=32663275&query_hl=1https://doi.org/10.1563/aaid-joi-D-19-00166
 43. Tallarico M, Meloni SM, Khanari E, Pisano M, Cochran DL. Minimally invasive sinus augmentation procedure using a dedicated hydraulic sinus lift implant device: a prospective case series study on clinical, radiologic, and patient-centered outcomes. *Int J Periodontics Restorative Dent.* 2017 2017;37(1):125–35. http://www.ncbi.nlm.nih.gov/entrez/query.fcgi?cmd=Retrieve&db=pubmed&dopt=Abstract&list_uids=27977827&query_hl=1https://doi.org/10.11607/prd.2914
 44. Dongo V, von Krockow N, Martins-Filho P, Weigl P. Lateral sinus floor elevation without grafting materials. Individual- and aggregate-data meta-analysis. *J Craniomaxillofac Surg.* 2018 2018;46(9):1616–24. http://www.ncbi.nlm.nih.gov/entrez/query.fcgi?cmd=Retrieve&db=pubmed&dopt=Abstract&list_uids=29980356&query_hl=1https://doi.org/10.1016/j.jcms.2018.06.012
 45. Okada T, Kawana H. Two-step procedure for the treatment of a maxillary sinus with complex sinus septa: a highly predictive method for sinus floor augmentation after perforation of the maxillary sinus membrane. *Int J Periodontics Restorative Dent.* 2019 2019;39(5):e175–80. http://www.ncbi.nlm.nih.gov/entrez/query.fcgi?cmd=Retrieve&db=pubmed&dopt=Abstract&list_uids=31449571&query_hl=1https://doi.org/10.11607/prd.3888
 46. Avila G, Wang HL, Galindo-Moreno P, Misch CE, Bagramian RA, Rudek I et al. The influence of the bucco-palatal distance on sinus augmentation outcomes. *J Periodontol.* 2010 2010;81(7):1041–50. http://www.ncbi.nlm.nih.gov/entrez/query.fcgi?cmd=Retrieve&db=pubmed&dopt=Abstract&list_uids=20450402&query_hl=1https://doi.org/10.1902/jop.2010.090686

Publisher's Note

Springer Nature remains neutral with regard to jurisdictional claims in published maps and institutional affiliations.